Solar Energy Materials & Solar Cells 143 (2015) 260–268

Contents lists available at ScienceDirect

Solar Energy Materials & Solar Cells

journal homepage: www.elsevier.com/locate/solmat

Towards the efficiency limits of silicon solar cells: How thin is too thin?

Piotr Kowalczewski *, Lucio Claudio Andreani

Department of Physics and CNISM, University of Pavia, via Bassi 6, I-27100 Pavia, Italy

ARTICLE INFO

Article history:
Received 11 May 2015
Received in revised form
17 June 2015
Accepted 29 June 2015
Available online 23 July 2015

Keywords:
Silicon solar cells
Efficiency limits
Device modelling
Auger recombination
Surface recombination
Light trapping

ABSTRACT

It is currently possible to fabricate crystalline silicon solar cells with the absorber thickness ranging from a few hundreds of micrometres (conventional wafer-based cells) to devices as thin as 1 μm. In this work, we use a model single-junction solar cell to calculate the limits of energy conversion efficiency and estimate the optimal absorber thickness. We have found that the limiting efficiency for cells in the thickness range between 40 and 500 μm is very similar and close to 29%. In this regard, we argue that decreasing the thickness below around 40 μm is counter-productive, as it significantly reduces the maximum achievable efficiency, even when an optimal light trapping is implemented. We analyse the roles of incomplete light trapping and extrinsic (bulk and surface) recombination mechanisms. For a reasonably high material quality, consistent with present-day fabrication techniques, the optimal thickness is always higher than a few tens of micrometres. We identify incomplete light trapping and parasitic losses as a major roadblock for improving the efficiency upon the current record of 25.6% for silicon solar cells. Finally, considering the main parameters that impact the solar cell performance, we quantify the requirements for achieving a given efficiency, which helps us to establish a proper design strategy for high efficiency silicon solar cells.

1. Introduction

In this work we focus on the efficiency limits of crystalline silicon (c-Si) solar cells. In this regard, we consider both ideal devices (perfect material and interfaces), as well as more realistic conditions, including defect-related recombinations, parasitic losses, and non-optimal light management. It is currently possible to fabricate c-Si solar cells with absorber thickness values that differ by two orders of magnitude. On the one end of the thickness range, there are conventional wafer-based c-Si solar cells with the absorber thickness of the order of a few hundreds of micrometres [1]. Epitaxial growth allows fabricating solar cells with the thickness of a few tens of micrometres [2]. Finally, epitaxy-free fabrication [3,4] makes possible fabricating c-Si solar cells with the absorbing layer as thin as 1 μm. For a proper design strategy, it is important to determine the optimal absorber thickness in terms of the energy conversion efficiency. We address this question using a model single-junction silicon solar cell.

It is well known that reducing the silicon thickness leads to the reduction of the total absorption, and thus of the photocurrent. This has to be compensated by implementing an appropriate light-trapping scheme. Yet, it should be emphasized that even when an optimal light trapping is applied (i.e., perfect anti-reflection action combined with a Lambertian scatterer), the maximum achievable absorption still decreases with decreasing material thickness [5,6]. On the other hand, V_{oc} generally tends to decrease with increasing thickness. For a given material quality, this leads to an optimal thickness that maximizes the conversion efficiency [6,7]. In this context, the goal of this work is twofold: First, to establish the most suitable thickness range for c-Si solar cells to approach the efficiency limits. Second, to identify the parameters that have to be improved in order to increase the energy conversion efficiency above the current record of 25.6% [8].

We use efficiency as a figure of merit to assess different solar cell structures. This is motivated by the fact that the cost of electricity is mainly determined by the efficiency, rather than by the cost of the active material (which, in the case of silicon, is constantly decreasing): cost of the active material is only a part of the cost of a photovoltaic module. This, in turn, is only a part of the total cost of a photovoltaic system. On the other hand, increasing the efficiency improves the performance of the whole system. In this regard, it is particularly important to estimate the optimal absorber thickness range that maximizes the efficiency. In our analysis we include intrinsic Auger recombination, as well as defect-based bulk and surface recombination mechanisms. We also introduce a simple approach that allows us to consider parasitic losses. We compare our results with the measured

* Corresponding author.
E-mail address: piotr.kowalczewski@unipv.it (P. Kowalczewski).

http://dx.doi.org/10.1016/j.solmat.2015.06.054
0927-0248/

performance of state-of-the-art silicon solar cells, showing the room for improvement in terms of current, voltage, and fill factor. We pay particular attention to parasitic losses, which we believe are the major roadblock in reaching efficiency above the current record of 25.6% [8].

A review of the efficiency limits of silicon solar cells is given in Ref. [9]. The limits reported in the literature [10–12] are usually calculated using the idealized diode equation [13]. This approach has the following limitations:

1. The diode equation gives less accurate results when the cell thickness is decreasing. We attribute this inaccuracy to the assumptions underlying the treatment of the space-charge region (SCR) in the idealized diode formalism. We further discuss the accuracy of the results obtained using the idealized diode equation in the Appendix.
2. Solar cells require selective contacts, which can be achieved using a p–n junction. Yet, the junction is not explicitly considered in the ideal diode approach. Therefore, the ideal diode equation gives unrealistic results that overestimate efficiency for undoped silicon.

Our approach allows us to overcome these limitations: we analytically obtain the photogeneration rate (ranging from double-pass absorption to Lambertian light trapping), explicitly consider a p–n junction, and numerically solve the drift–diffusion equations. This allows us to calculate more realistic efficiency limits of silicon solar cells in a wide range of cell thicknesses and doping levels.

The paper is organized as follows: in Section 2 we describe our approach, based on an analytical photogeneration rate and numerical solution of the drift–diffusion equations. In Section 3 we calculate the efficiency limits of c-Si solar cells. In Section 4 we discuss the effects of incomplete light trapping. In Section 5 we cover the impact of bulk material imperfections on the cell performance, and we introduce a simple approach to include parasitic losses in the analysis. In Section 6 we discuss the role of surface recombination. In Section 7 we quantify the requirements, in terms of bulk and surface material quality, to achieve a given efficiency. Conclusions are given in Section 8. Finally, in the Appendix we compare the results of our numerical treatment with those obtained using the idealized diode equation.

2. Numerical approach

Let us consider the structure sketched in Fig. 1. It consists of a 5 nm thick n-type emitter and a p-type base of variable thickness. Such a thin emitter minimizes recombination losses in this heavily doped layer. To calculate the efficiency limits we assume no reflection at the front interface, a perfect back reflector (BR), and a Lambertian light trapping [14,15]. In Fig. 1 we schematically show the Lambertian scatterer at the front, yet we note that the structure considered in the calculations is one-dimensional, and the photogeneration rate as a function of depth is calculated analytically. Finally, we assume full-area contacts: the carriers are collected at the silicon/BR and emitter/transparent front contact interfaces. With these simplifying assumptions, we will be able to draw general conclusions, not related to a particular solar cell structure.

The photogeneration rate corresponding to the Lambertian limit is calculated as a function of energy and depth, according to Ref. [6]:

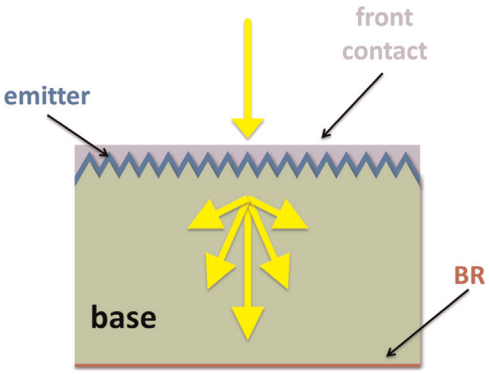

Fig. 1. Investigated solar cell structure consisting of a 5 nm thick n-type emitter (the blue region), p-type base (the green region), and a perfect back reflector (BR), which also serves as a back contact. The front surface is textured so that the incident light is scattered and trapped within the absorber. (For interpretation of the references to colour in this figure caption, the reader is referred to the web version of this paper.)

$$G_{\mathrm{LL}}(z,E)=\frac{\alpha_{\mathrm{lt}}\left(R_{\mathrm{b}}e^{-2\alpha_{\mathrm{lt}}W}e^{\alpha_{\mathrm{lt}}z}+e^{-\alpha_{\mathrm{lt}}z}\right)}{1-e^{-2\alpha_{\mathrm{lt}}W}\left(1-\frac{1}{n_{\mathrm{Si}}^2}\right)}\times\phi_{\mathrm{AM1.5G}}, \tag{1}$$

where n_{Si} is the refractive index of c-Si [16] and $\phi_{\mathrm{AM1.5G}}$ is the photon flux density corresponding to the AM1.5G solar spectrum [17]. The effective absorption coefficient α_{lt} is related to the light path enhancement in textured cells according to Ref. [15]. In the literature we can find a number of different strategies that allow approaching the Lambertian limit, including ordered [5,18–20] and quasi-ordered [21–23] photonic structures, as well as random textures [24–27].

The photogeneration rate calculated using Eq. (1) is integrated with respect to energy (over the solar spectrum) and used as the generation term in the drift–diffusion equations, which are solved using Finite-Element Method (FEM). We use FEM implemented in the commercial device simulator Silvaco Atlas [28]. This methodology is similar to the one described in our previous works [7,29].

3. Efficiency limits

We start by considering solar cells limited by intrinsic Auger recombination. We treat Auger recombination using the parametrization reported by Richter et al. [30]. In our calculations we assume that front and back surface recombination velocities are equal to 1 cm/s, unless specified otherwise. We also consider band gap narrowing (BGN) according to the model by Schenk [31]. Finally, we neglect free carrier absorption, which is a second-order effect [10,12]. Silicon is an indirect band gap material, and thus we also neglect losses related to radiative recombination, which may give an appreciable effect only for very thick cells. Yet, for the thick cells the probability of photon recycling increases [11], i.e., radiatively emitted photons are reabsorbed. These two effects are likely to compensate each other. In the Appendix we show that radiative recombination together with photon recycling have a negligible effect on the cell performance.

In Fig. 2(a) we show the limiting efficiency of c-Si solar cells as a function of the absorber thickness, calculated for the structure sketched in Fig. 1. For each thickness, we have simultaneously optimized the emitter and base doping (the doping profile in each layer is assumed to be constant). The efficiency as a function of emitter doping N_{d} has a wide maximum, and the optimal value $N_{\mathrm{d}}=1.5\times10^{18}\ \mathrm{cm}^{-3}$ does not change with the absorber thickness,

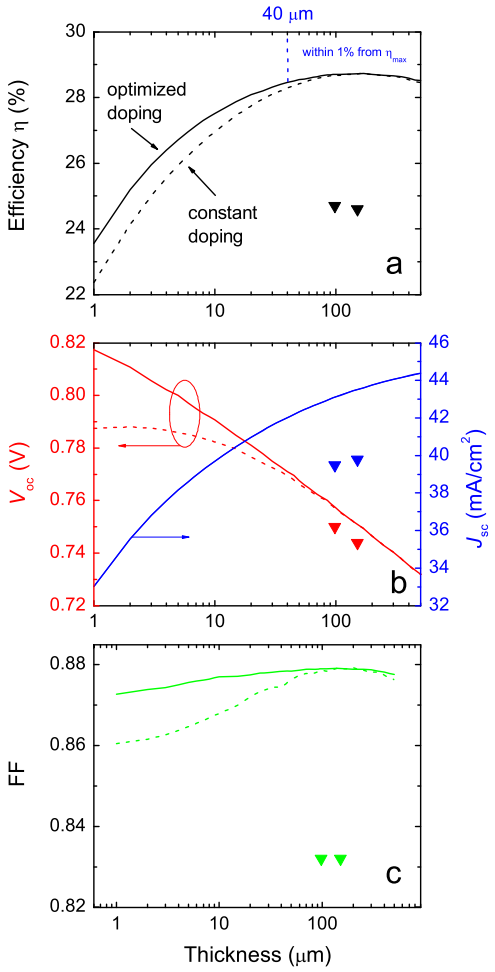

Fig. 2. (a) The limiting efficiency of c-Si solar cells as a function of the absorber thickness. (b) V_{oc} and J_{sc}, and (c) fill factor (FF) corresponding to the calculated efficiency limits. The solid lines are calculated by optimizing the base doping for each thickness, whereas the dashed lines are calculated assuming a constant doping $N_a = 10^{16}$ cm^{-3}. The triangles denote the performance of the record-efficiency HIT cells [32].

as the emitter thickness itself is kept constant. Regarding the base doping N_a, the solid lines in Fig. 2 are calculated by optimizing N_a for each thickness. On the other hand, the dashed lines are calculated assuming a constant doping $N_a = 10^{16}$ cm^{-3}, which is the optimal doping for the optimal absorber thickness equal to 170 μm. The optimal base doping is highest for thinner cells (reaching 10^{17} cm^{-3} for the 1 μm thick cell) and decreases with increasing thickness.

The maximum efficiency is equal to η_{max}=28.73%, and it is obtained for the 170 μm thick cell. This is lower than the efficiency limit of 29.43% reported recently in the literature [12]. The main reason is that in our calculations, the base doping increases Auger losses and therefore reduces the efficiency. On the contrary, the limit reported in the literature has been obtained using the idealized diode equation and assuming undoped silicon, as explained in Section 1 and in the Appendix.

We note that the efficiency as a function of the absorber thickness has a broad maximum, and even a small change in the input parameters can substantially shift the nominal optimal thickness. In the range between 40 and 500 μm, the calculated efficiency differs by no more than 1% (relative units) from η_{max}. This somehow arbitrary interval shows that for thickness values that differ considerably (by one order of magnitude), the maximum achievable efficiency is very similar. Finally, for an absorber thickness below 40 μm, the efficiency drops significantly.

These results are compared with the efficiencies of the state-of-the-art HIT cells [32] (the triangles). We note that the efficiency of the HIT solar cell has been recently increased to 25.6% [8]. Yet, the thickness of the record cell is not specified, and therefore we were unable to include it in Fig. 2. This analysis shows that the theoretical margin for improvement of single-junction silicon solar cells is around 3% (absolute units).

In Fig. 2(b) we show V_{oc} and J_{sc}, and in Fig. 2(c) fill factor corresponding to the calculated efficiency limits. The base doping optimization allows us to slightly improve V_{oc}, whereas J_{sc} is practically the same. Comparing these results with the performance of the HIT cells, we can see that for both values of thickness (98 and 151 μm), the measured value is around 99% of the limiting V_{oc}, around 94.6% of the limiting FF, and around 91.6% of the limiting J_{sc}. This analysis indicates that these cells are limited by, in decreasing order of significance, J_{sc}, FF, and V_{oc}. This suggests that optimizing light trapping and, especially, minimizing optical parasitic losses (affecting J_{sc}), as well as improving the contacts (affecting FF) is the key to further increase the efficiency towards the limiting values.

Open-circuit voltage and short-circuit current exhibit the opposite trends as a function of the absorber thickness. It is well known that reducing the absorber thickness decreases the photocurrent [5], even when a Lambertian light trapping is implemented. This current loss is not compensated by the voltage gain. Therefore, decreasing the absorber thickness below a few tens of micrometres is counter-productive from the point of view of efficiency. We note that the relative scales in Fig. 2 are different: in the considered thickness range, V_{oc} changes by around 7%, J_{sc} by around 34%, and FF by around 2%.

To further elaborate the issue of the base doping optimization, in Fig. 3 we show the efficiency as a function of the base doping and absorber thickness. This plot can be compared with the results presented in Fig. 4 reported in Ref. [12], which are obtained using the idealized diode equation. In the case of the diode equation, solar cells approach the limiting efficiency for a practically undoped silicon. Yet, in our calculations we can see a clear maximum around 10^{16} cm^{-3} (for the thickness range around 100–200 μm). Then, efficiency decreases with decreasing doping. This difference is due to the fact that the junction is not explicitly considered in the ideal diode approach. Therefore, the requirement of selective contacts, which can be achieved using a p–n junction, is not included. This leads to unrealistic results for very lightly doped materials. Finally, the optimal value of the base doping calculated above is similar to the typical values reported in the literature, e.g., 10^{16} cm^{-3} quoted in Ref. [13].

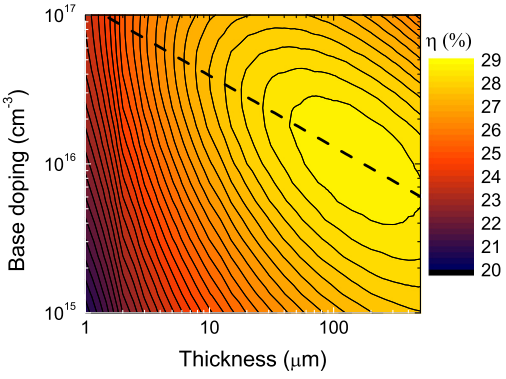

Fig. 3. Efficiency as a function of the base doping and absorber thickness. The dashed line indicates the optimal doping.

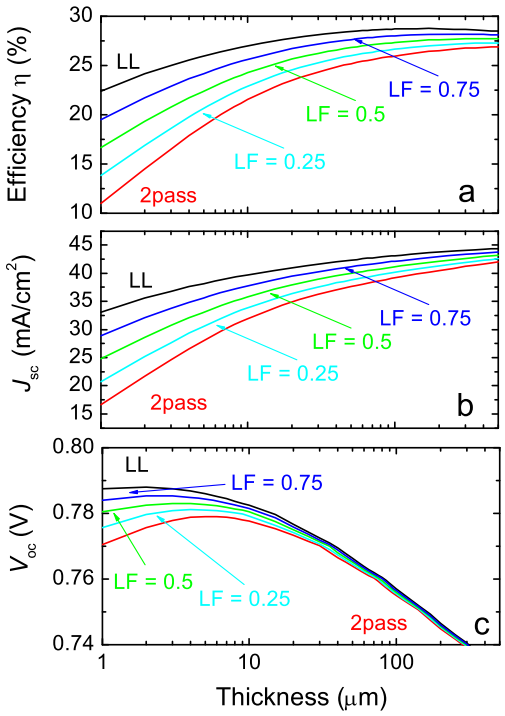

Fig. 4. (a) Efficiency, (b) short-circuit current J_{sc}, and (c) open-circuit voltage V_{oc} calculated as a function of the absorber thickness for different values of the light-trapping factor LF.

We perform the base doping optimization considering intrinsic Auger recombination, which is proportional to the carrier concentration. This allows us to calculate the efficiency limits of the considered solar cells. Nevertheless, when additional (extrinsic) loss mechanisms are included, the optimal value of the base doping may change.

For the simplicity of the analysis, in the rest of this paper we assume a constant base doping $N_a = 10^{16}$ cm^{-3}.

4. Effects of incomplete light trapping

In the calculations above we have assumed a Lambertian light trapping, which is often taken as a benchmark in the optical design of solar cells. Yet, it is difficult to fulfill this assumption in realistic devices. Therefore, let us now focus on the role of light trapping in achieving the efficiency limits. To do so, we consider solar cells with incomplete light trapping: the photogeneration rate is taken as a weighted average of the photogeneration G_{2p}, corresponding to the double-pass absorption (i.e., unstructured cell) and the photogeneration G_{LL} corresponding to the Lambertian limit. G_{2p} is calculated as

$$G_{2p}(z, E) = \alpha\left(e^{-z\alpha} + e^{-(2w-z)\alpha}\right) \times \phi_{AM1.5G}, \quad (2)$$

where α is the absorption coefficient of c-Si [16]. As previously, also in the double-pass case we assume a perfect back reflector and anti-reflection action. We note that there are no interference effects included in Eq. (2). When we consider single wavelengths, the interference effects are profound. Yet, when we integrate the photogeneration rate over the solar spectrum, the interference peaks are smeared out, which justifies the approximation used in Eq. (2). The resulting weighted photogeneration rate is calculated as

$$G(z) = P_{loss} \times \left[(1 - LF) \times G_{2p}(z) + LF \times G_{LL}(z)\right], \quad (3)$$

where LF is the light-trapping factor: LF=0 corresponds to the double-pass case, whereas LF=1 corresponds to the Lambertian limit. G is a function of depth z. Finally, P_{loss} is a factor related to reflection at the front interface and to parasitic optical losses. For simplicity, we assume that P_{loss} does not depend on wavelength.

We begin by assuming no parasitic losses, that is $P_{loss} = 1$. In Fig. 4(a) we demonstrate that light trapping increases the maximum achievable efficiency. This is not the case for semiconductors with a direct energy band-gap, like GaAs, where surface texturing does not increase the maximum achievable efficiency [33]. Therefore, for silicon solar cells light trapping is an essential element required to approach the efficiency limits, even for very thick cells.

As expected, light trapping significantly increases J_{sc}, which is shown in Fig. 4(b). J_{sc} for the thickest cells does not saturate because of a small absorption below the energy band-gap. Moreover, Fig. 4(c) shows that light trapping also slightly improves V_{oc}. Yet, this effect is appreciable only for cell thicknesses below 10 μm, that is in a thickness range which is not particularly promising for achieving high efficiency. V_{oc} as a function of the thickness for the double-pass case exhibits a gentle maximum. This may be partly because the base doping is not optimized for thin cells.

Although the importance of light trapping for maximizing the conversion efficiency of c-Si solar cells is well known, the present results allow us to quantify the effects of incomplete light trapping on the efficiency. Moreover, Eq. (3) represents a simple model that can be also used to study the effects of parasitic losses, which are different from the effects related to incomplete light trapping. We shall discuss it in more detail in the next section.

5. Material imperfections and parasitic losses

So far, we have considered an idealized material, and therefore the cell performance was limited by intrinsic Auger recombination. Let us now consider extrinsic losses related to defect-base SRH recombination and parasitic optical losses.

With the emitter as thin as 5 nm, the cell efficiency is likely to be limited by the diffusion length $L_{n,SRH}$ of the minority carriers (electrons) in the base. In Fig. 5(a) we show the efficiency as a function of the absorber thickness and $L_{n,SRH}$, calculated for the structure with a Lambertian light trapping. The diffusion length of holes in the highly doped emitter is taken equal to $L_{p,SRH}=L_{n,SRH}/10$. It can be seen that thicker cells are more sensitive to SRH recombination. In this regard, thinner cells with the absorber thickness of around 40 μm can reach nearly the same η_{max} as the thicker cells, but the conditions in terms of the absorber quality are relaxed. Finally, reducing the absorber quality (i.e., decreasing $L_{n,SRH}$) shifts the optimal thickness towards thinner cells.

Results shown in Fig. 5(b) are calculated including parasitic losses $P_{loss}=0.9$. We estimate that this is approximately the level of parasitic losses in the HIT cells discussed above. The trends are similar to those calculated assuming $P_{loss}=1$, yet the maximum achievable efficiency is proportionally decreased. Moreover, for a given efficiency level, the optimal thickness is increased.

The results of Fig. 5 allow us to estimate the optimal thickness and the required material quality to reach a given efficiency level. For example, to surpass 26% efficiency, in the idealized case of no parasitic losses and a complete (Lambertian) light trapping, we need an electron diffusion length of around 1 mm. In the more realistic case, when parasitic losses are included (say, $P_{loss}=0.9$),

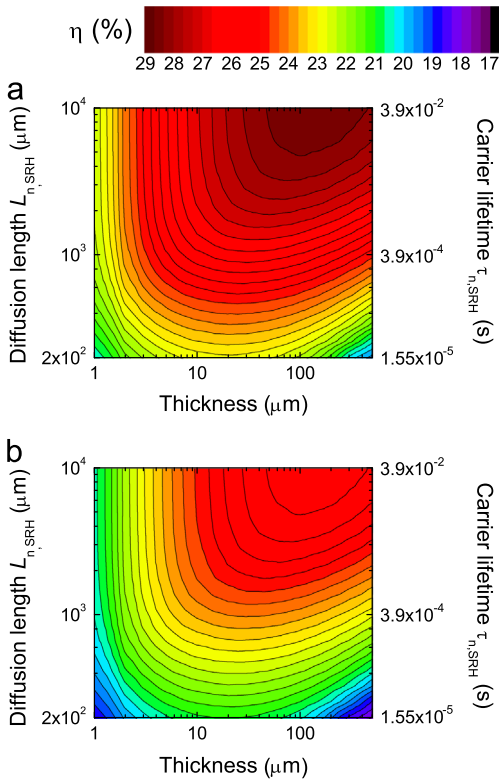

Fig. 5. (a) Efficiency as a function of the thickness and diffusion length $L_{n,SRH}$ of the minority carriers (electrons) in the base, calculated for the structures with a Lambertian light trapping. (b) The same quantity but including factor related to parasitic losses $P_{loss} = 0.9$. We note that $L_{n,SRH}$ is related to SRH recombination, originating from defects in the base. The scale on the right shows the corresponding carrier lifetime.

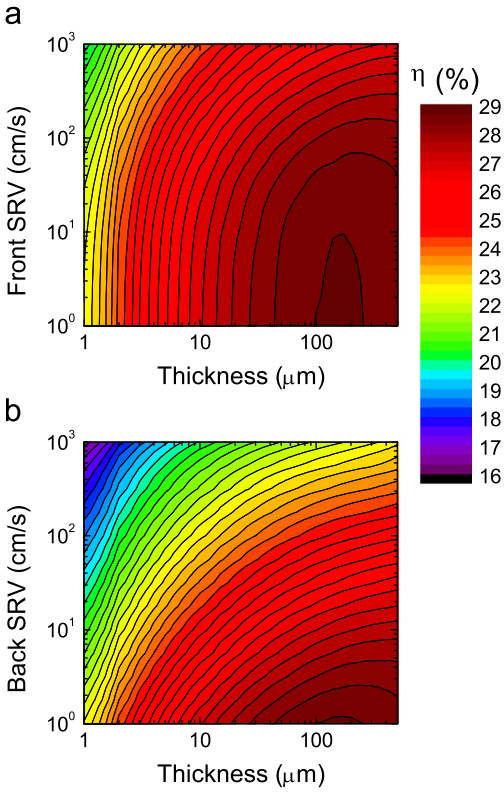

Fig. 6. Efficiency as a function of (a) front and (b) back surface recombination velocity (SRV), and of the absorber thickness. For the bulk transport losses, we assume only Auger recombination.

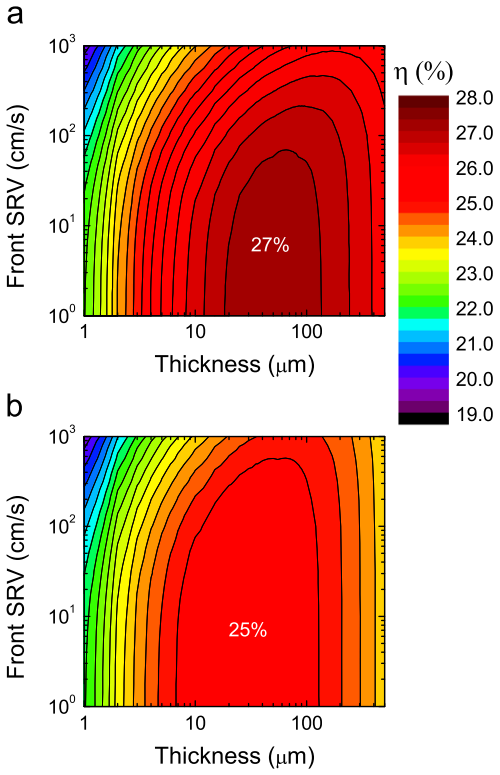

Fig. 7. Efficiency as a function of front surface recombination velocity (SRV) and the absorber thickness. For bulk transport losses, we assume Auger and SRH recombination. The material quality (i.e., $L_{n,SRH}$) is reduced, so that the maximum achievable efficiency is 27% for $L_{n,SRH} \approx 1768$ μm (a) and 25% for $L_{n,SRH} \approx 675$ μm (b).

achieving efficiency above 26% requires a diffusion length higher than ≈4 mm for an optimal thickness of ≈50 μm.

6. Surface recombination

Let us now estimate the constraints on the efficiency imposed by surface recombination, which is another extrinsic loss mechanism, related to defect states at the surface. In Fig. 6 we show the efficiency as a function of (a) front and (b) back surface recombination velocity (SRV), and of the absorber thickness. At first, for the bulk transport losses we assume only Auger recombination. It can be seen that approaching the efficiency limits requires SRV to be less than a few cm/s, with solar cells being more sensitive to recombination at the rear interface rather than to recombination at the front.

In the calculations above, we assumed a perfect material quality. Yet, in our previous work we have demonstrated that the importance of surface recombination depends on bulk recombination rate, i.e., the higher is the material quality, the more important are losses at the surface [7]. From now on we focus on front surface recombination, neglecting recombination at the back, which has anyway to be of the order of a few cm/s to target high efficiency. In realistic devices, there is usually an oxide passivating layer and point contacts at the back side. For this reason, back SRV can be significantly reduced. On the other hand, front SRV may be increased due to texturing.

In Fig. 7 we plot the efficiency as a function of front surface recombination velocity (SRV) and absorber thickness. For bulk transport losses, we assume Auger and SRH recombination. We adjust the diffusion length $L_{n,SRH}$ of the minority carriers (electrons) in the base, so that the maximum achievable efficiency is

reduced to a certain value. This kind of analysis allows us to answer the following question: Having a given material quality, what is the maximum allowed value of front SRV to achieve the limiting efficiency?

In Fig. 7(a) the maximum possible efficiency is around 27%, which is obtained for $L_{n,SRH} \approx 1768$ μm. With this material quality, the optimal absorber thickness is 40 μm, and the efficiency of 27% can be achieved for the thickness range between 20 and 80 μm. In this case, front SRV should be below a few tens of cm/s.

In Fig. 7(b) we further reduce diffusion length to $L_{n,SRH} \approx 675$ μm, so that the maximum possible efficiency is around 25%. The region of the highest efficiency (25% or slightly above) is clearly wider than in the previous plot. Also the conditions for surface recombination at the front interface are relaxed: in this case, front SRV should be below a few hundreds of cm/s. This analysis confirms that the impact of surface recombination decreases with decreasing material quality.

7. Requirements for approaching the efficiency limits

To summarize the results presented in this paper, in this section we estimate the requirements for approaching a given energy conversion efficiency. In this regard, we analyse both bulk material quality (related to diffusion length of electrons in the base $L_{n,SRH}$) and quality of the surfaces (related to surface recombination velocity).

In Fig. 8(a) we show the diffusion length of electrons in the base $L_{n,SRH}$ as a function of the maximum achievable efficiency, whereas Fig. 8(b) indicates the corresponding (optimal) thickness of the absorbing layer. These results are extracted from Fig. 5, i.e.,

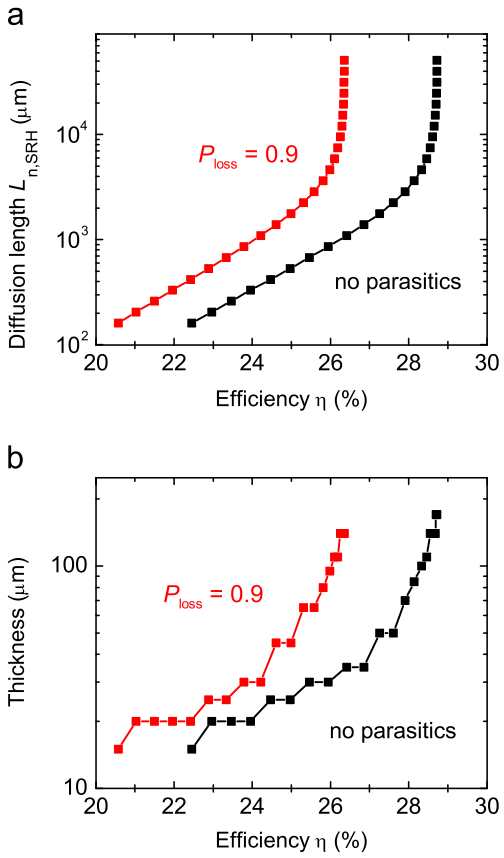

Fig. 8. (a) Diffusion length of electrons in the base $L_{n,SRH}$ as a function of the maximum achievable efficiency. (b) Corresponding (optimal) thickness of the absorbing layer.

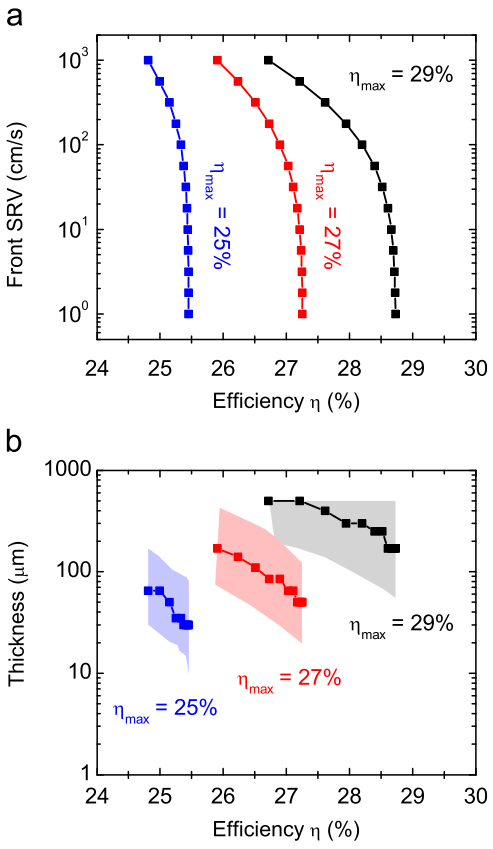

Fig. 9. (a) Front surface recombination velocity (SRV) as a function of the maximum achievable efficiency. (b) Corresponding optimal thickness of the absorbing layer. We consider cells limited by Auger recombination (the black lines), as well as cells with SRH recombination: $L_{n,SRH} \approx 1768$ μm with the maximum achievable efficiency of around 27% (the red lines) and $L_{n,SRH} \approx 675$ μm with the maximum achievable efficiency of around 25% (the blue lines). The colour regions indicate 1% (relative) tolerance intervals for each material quality. (For interpretation of the references to colour in this figure caption, the reader is referred to the web version of this paper.)

for each $L_{n,SRH}$ we have extracted the maximum achievable efficiency and the corresponding cell thickness.

In Fig. 8(a) we can distinguish two trends. In the case of no parasitic losses (black line), for the efficiency range below around 28%, $L_{n,SRH}$ and the corresponding maximum achievable efficiency scale linearly. Yet, above 28%, significant increase of $L_{n,SRH}$ gives only a minor, if any, improvement of efficiency.

The red line in Fig. 8(a) shows the results calculated including parasitic losses, that is P_{loss}=0.9. Parasitic losses result in a shift of the red curve towards lower efficiencies, with the maximum efficiency of around 26%.

We can also see that the optimal absorber thickness changes significantly in the considered efficiency range, as shown in Fig. 8 (b). For small $L_{n,SRH}$, the optimal thickness is of the order of a few tens of micrometres. Then, with increasing $L_{n,SRH}$, the optimal thickness increases rapidly, reaching around 170 μm for $L_{n,SRH}$ of the order of millimetres.

A similar analysis can be performed regarding surface recombination. In Fig. 9(a) we show front surface recombination velocity (SRV) as a function of the maximum achievable efficiency, and in Fig. 9(b) we show the corresponding optimal thickness of the absorbing layer. These results have been extracted from Figs. 6 and 7.

We consider cells limited by Auger recombination (the black lines), as well as cells with SRH recombination: $L_{n,SRH} \approx 1768$ μm with the maximum achievable efficiency of around 27% (the red lines) and $L_{n,SRH} \approx 675$ μm with the maximum achievable

efficiency of around 25% (the blue lines). In general, the cells are fairly insensitive to recombination at the front interface if SRV is below a few hundreds of cm/s. This is of the order of magnitude of the effective SRV, currently measured for nanostructured solar cells [34]. Moreover, increasing SRV increases the optimal absorber thickness, as thinner cells are more sensitive to surface recombination.

As pointed out previously, efficiency as a function of the absorber thickness exhibits a wide maximum. For this reason, in Fig. 9(b) we include tolerance intervals for each material quality. The intervals are indicated by the colour regions, and show thickness range in which efficiency changes by no more than 1% relative. For example, if we consider Auger-limited cells (the black lines), and assume front SRV equal to 100 cm/s, we can see that the efficiency changes by no more than 1% relative in the thickness range from 80 to 500 μm. We note that the calculations are performed up to 500 μm (which we consider a practical limit for fabrication).

The results presented above show that the optimal absorber thickness is determined by an interplay between bulk and surface losses. Nevertheless, for a reasonably high bulk and surface quality (consistent with present-day fabrication techniques), an optimal thickness is always above 100 μm. Therefore, the conclusion that decreasing the absorber thickness below a few tens of micrometres is counter-productive holds for a wide range of material parameters.

8. Conclusions

In conclusion, we have presented an electro-optical analysis of the limiting efficiency of c-Si solar cells, considering a wide range of material parameters. We performed our study using a model one-dimensional solar cell. This allowed us to draw general conclusions, not related to a particular solar cell structure. When more realistic structures are considered, the calculated performance may change but the trends are likely to remain the same.

In our numerical framework, we take the analytical photogeneration rate (assuming full or partial light trapping) and numerically solve the drift–diffusion equations to obtain the cell performance. This gives a realistic description of carrier dynamics in the device and allows us to easily introduce intrinsic and extrinsic loss mechanisms. Moreover, our approach overcomes a number of simplifications present in the calculations of the efficiency limits previously reported in the literature. Most importantly, we explicitly consider a p–n junction, which is particularly important in the case of thin cells, when the junction region is a significant part of the whole cell. The detailed comparison between our method and the diode model can be found in the Appendix.

Comparison with the HIT structures suggests that silicon solar cells are limited by (in decreasing order of significance) J_{sc}, FF, and V_{oc}. Thus, improving J_{sc} (via light trapping and reducing parasitic losses) and FF (by improving the quality of contacts) seems to be the key to further boost the performance beyond the current efficiency record.

In the first part of this contribution, we calculated the efficiency limits of c-Si solar cells. Therefore, we focused on the cells limited by intrinsic Auger recombination. We have demonstrated that the limiting efficiency as a function of the absorber thickness exhibits a wide maximum: 40 μm thick cell can be nearly as efficient as the solar cell with the optimal absorber thickness (around 170 μm). It is therefore more practical to consider the *optimal thickness range*, rather than a single optimal thickness. In this regard, we argued that decreasing the thickness below around 40 μm is counter-productive, as it significantly reduces the maximum achievable efficiency.

When extrinsic SRH recombination is considered, we notice that thicker cells are more sensitive to bulk losses, and therefore the conditions to reach the limiting efficiency for thinner cells are relaxed. Yet, including surface recombination shows the opposite trend: thicker cells are less sensitive to surface recombination, as the surface-to-volume ratio is reduced. Nevertheless, for a reasonably high bulk and surface quality, it remains true that decreasing the thickness below a few tens of micrometres is counter-productive in terms of the efficiency.

The current efficiency record for single junction silicon solar cells is 25.6% [8,35]. Detailed experimental study would be necessary to indicate the major roadblock for going above this value. Nevertheless, our analysis suggests that the dominant loss mechanisms in the state-of-the-art cells are related to the current loss. Therefore, reducing parasitic losses seems to be necessary to increase the efficiency above 26%. Achieving the efficiency above 27% puts severe constraints on surface recombination. Finally, increasing the efficiency above the calculated limit for single junction c-Si solar cells requires novel technologies, like silicon-perovskite tandem structures [36–39].

Acknowledgements

This work was supported by the EU through Marie Curie Action FP7-PEOPLE-2010-ITN Project no. 264687 "PROPHET". The authors are grateful to Angelo Bozzola for carefully reading the manuscript and, together with Marco Liscidini, for many fruitful discussions.

Appendix A. Comparison with the idealized diode equation

The efficiency limits of silicon solar cells are usually calculated using the idealized diode equation [12]:

$$J(V) = J_L - qWR, \tag{A.1}$$

where J_L is the photogenerated current density, W is the cell thickness, and R is the total bulk recombination rate. In this Appendix, we elaborate on the difference between the results obtained using Eq. (A.1) and numerical solution of the drift–diffusion equations by means of finite-element approximation.

In Fig. A1 we show (a) efficiency η, (b) open-circuit voltage V_{oc}, (c) short-circuit current J_{sc}, and (d) fill factor FF as a function of the absorber thickness. The red dashed lines refer to the results obtained using the idealized diode equation, whereas the black lines denote the results obtained by solving the drift–diffusion equations by means of finite-element approximation. The material parameters and recombination models are the same in both approaches: we include Auger recombination according to Richter et al. [30] and BGN according to the model by Schenk [31].

By performing the calculations using Eq. (A.1), we aim at reproducing the results reported in Ref. [12]. In Fig. A1(a) we compare our calculations of efficiency with the results presented in the reference work. The results obtained using Eq. (A.1) are very close to the results digitized from Ref. [12]. We attribute small discrepancies to the fact that in our calculations we neglect free-carrier absorption and photon recycling: as discussed above, these two effects are likely to compensate each other, and indeed their impact on the cell performance is negligible. For this reason, we have also neglected these effects in the calculations presented in the main part of this paper. Finally, the calculations presented in this work are performed at temperature $T=300$ K, whereas the results in the reference work are performed at $T=25^\circ$ C.

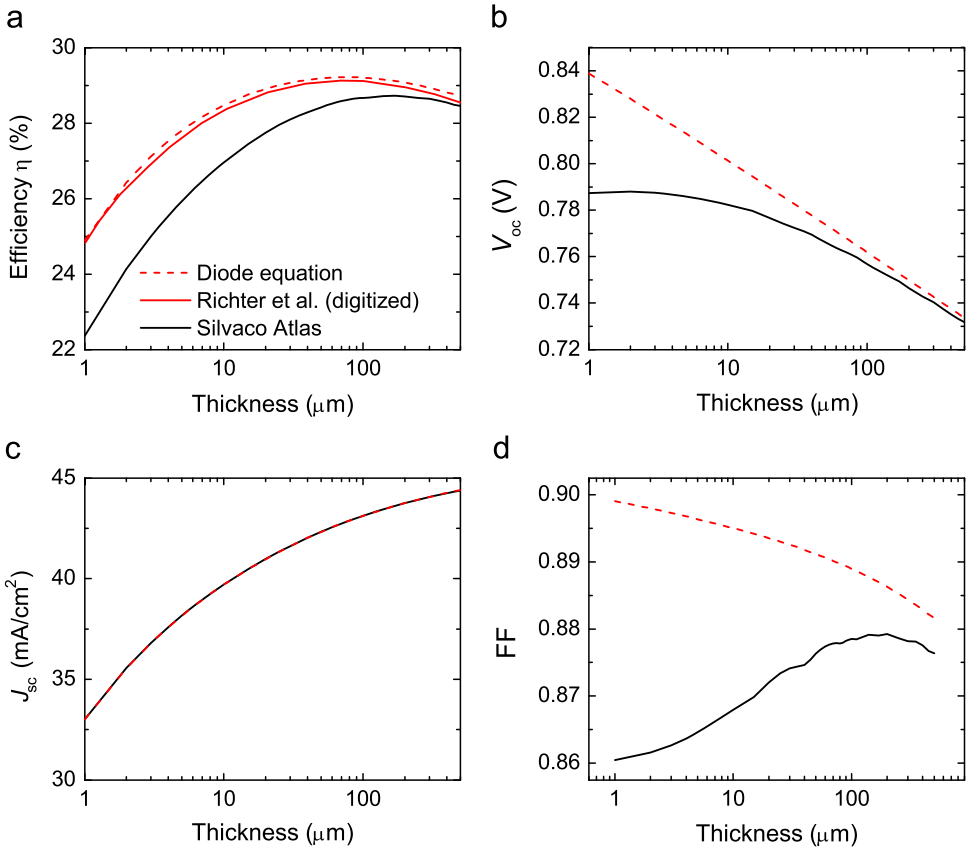

Fig. A1. (a) Efficiency η, (b) open-circuit voltage V_{oc}, (c) short-circuit current J_{sc}, and (d) fill factor FF as a function of the absorber thickness. The red dashed lines refer to the results obtained using the idealized diode equation, whereas the black lines refer to the results obtained by solving the drift–diffusion equations by means of finite-element approximation. In (a) we show the comparison with the results digitized from Ref. [12]. (For interpretation of the references to colour in this figure caption, the reader is referred to the web version of this paper.)

The discrepancy between the results obtained using Eq. (A.1) and the full numerical simulations increases with decreasing absorber thickness. In the limiting case of very thick cells, both approaches give essentially the same results. Yet, the difference in efficiency for 1 μm thick cell is around 2% (absolute value), i.e., the ideal diode treatment gives higher values. Since J_{sc} calculated using both approaches is the same[1], we can trace the discrepancy back to the difference in V_{oc} and fill factor: V_{oc} calculated using Eq. (A.1) increases linearly with decreasing thickness, whereas V_{oc} obtained from the full numerical simulations tends to saturate. Moreover, FF calculated using Eq. (A.1) increases with decreasing absorber thickness, whereas FF obtained from the full numerical simulations shows the opposite trend (small fluctuations may be due to numerical inaccuracy).

We can therefore conclude that the results obtained using the idealized diode equation become less accurate with decreasing absorber thickness, i.e., in this approach the efficiency for thin cells is overestimated. We tentatively attribute this inaccuracy to the intrinsic limitations of the diode equation, in particular to the assumptions underlying the treatment of the space-charge region (SCR) in the idealized diode formalism: the idealized diode equation can be derived from the drift–diffusion equations assuming that there is no carrier generation nor recombination in SCR [40]. It means that the currents in SCR are constant. With the assumed doping concentrations, the width of SCR is around 350 nm. Therefore, if the cells are thick, SCR is only a small part of the whole cell. Yet, in the case of thin cells, SCR is a significant part of the whole cell, and the assumption that there is no carrier generation nor recombination in SCR seriously disturbs the current distribution in the cell.

[1] The fact that J_{sc} is the same in both cases also confirms that the mesh used in the finite-element calculations is dense enough to properly reproduce the photogeneration profile.

References

[1] J. Zhao, A. Wang, M.A. Green, F. Ferrazza, 19.8% efficient honeycomb textured multicrystalline and 24.4% monocrystalline silicon solar cells, Appl. Phys. Lett. 73 (1998) 1991.

[2] J.H. Petermann, D. Zielke, J. Schmidt, F. Haase, E.G. Rojas, R. Brendel, 19%-efficient and 43 μm-thick crystalline Si solar cell from layer transfer using porous silicon, Prog. Photovoltaics: Res. Appl. 20 (1) (2012) 1–5.

[3] X. Meng, V. Depauw, G. Gomard, O. El Daif, C. Trompoukis, E. Drouard, C. Jamois, A. Fave, F. Dross, I. Gordon, C. Seassal, Design, fabrication and optical characterization of photonic crystal assisted thin film monocrystalline-silicon solar cells, Opt. Express 20 (104) (2012) A465–A475.

[4] C. Trompoukis, O. El Daif, V. Depauw, I. Gordon, J. Poortmans, Photonic assisted light trapping integrated in ultrathin crystalline silicon solar cells by nanoimprint lithography, Appl. Phys. Lett. 101 (10) (2012) 103901.

[5] A. Bozzola, M. Liscidini, L.C. Andreani, Photonic light-trapping versus Lambertian limits in thin film silicon solar cells with 1D and 2D periodic patterns, Optics Express 20 (102) (2012) A224–A244.

[6] A. Bozzola, P. Kowalczewski, L. Andreani, Towards high efficiency thin-film crystalline silicon solar cells: the roles of light trapping and non-radiative recombinations, J. Appl. Phys. 115 (9) (2014) 094501.

[7] P. Kowalczewski, A. Bozzola, M. Liscidini, L.C. Andreani, Light trapping and electrical transport in thin-film solar cells with randomly rough textures, J. Appl. Phys. 115 (19) (2014) 194504.

[8] Panasonic HIT Solar Cell Achieves World's Highest Energy Conversion Efficiency of 25.6% at Research Level, ⟨http://panasonic.co.jp/corp/news/official.data/data.dir/2014/04/en140410-4/en140410-4.html⟩, Panasonic Press Release, 10 April 2014 (accessed 28 August 2014).

[9] R.M. Swanson, Approaching the 29% limit efficiency of silicon solar cells, in: Conference Record of the 31st IEEE Photovoltaic Specialists Conference, 2005, IEEE, 2005, pp. 889–894.

[10] T. Tiedje, E. Yablonovitch, G.D. Cody, B.G. Brooks, Limiting efficiency of silicon solar cells, IEEE Trans. Electron Devices 31 (5) (1984) 711–716.
[11] M.J. Kerr, A. Cuevas, P. Campbell, Limiting efficiency of crystalline silicon solar cells due to Coulomb-enhanced Auger recombination, Prog. Photovoltaics: Res. Appl. 11 (2) (2003) 97–104.
[12] A. Richter, M. Hermle, S. Glunz, Reassessment of the limiting efficiency for crystalline silicon solar cells, IEEE J. Photovoltaics 3 (4) (2013) 1184–1191.
[13] J. Nelson, The Physics of Solar Cells, Imperial College Press, London, 2003.
[14] E. Yablonovitch, Statistical ray optics, J. Opt. Soc. Am. 72 (7) (1982) 899–907.
[15] M.A. Green, Lambertian light trapping in textured solar cells and light-emitting diodes: analytical solutions, Prog. Photovoltaics: Res. Appl. 10 (4) (2002) 235–241.
[16] M.A. Green, Self-consistent optical parameters of intrinsic silicon at 300k including temperature coefficients, Sol. Energy Mater. Sol. Cells 92 (11) (2008) 1305–1310.
[17] Reference Solar Spectral Irradiance: Air Mass 1.5, ⟨http://rredc.nrel.gov/solar/spectra/am1.5/⟩.
[18] A. Abass, K.Q. Le, A. Alu, M. Burgelman, B. Maes, Dual-interface gratings for broadband absorption enhancement in thin-film solar cells, Phys. Rev. B 85 (11) (2012) 115449.
[19] O. Isabella, S. Solntsev, D. Caratelli, M. Zeman, 3-D optical modeling of thin-film silicon solar cells on diffraction gratings, Prog. Photovoltaics: Res. Appl. 21 (1) (2013) 94–108.
[20] G. Gomard, R. Peretti, E. Drouard, X. Meng, C. Seassal, Photonic crystals and optical mode engineering for thin film photovoltaics, Opt. Express 21 (103) (2013) A515–A527.
[21] R. Peretti, G. Gomard, L. Lalouat, C. Seassal, E. Drouard, Absorption control in pseudodisordered photonic-crystal thin films, Phys. Rev. A 88 (5) (2013) 053835.
[22] E.R. Martins, J. Li, Y. Liu, V. Depauw, Z. Chen, J. Zhou, T.F. Krauss, Deterministic quasi-random nanostructures for photon control, Nat. Commun. 4 (2013) 2665.
[23] A. Bozzola, M. Liscidini, L.C. Andreani, Broadband light trapping with disordered photonic structures in thin-film silicon solar cells, Prog. Photovoltaics: Res. Appl. 22 (2013) 1237–1244.
[24] K. Jäger, M. Fischer, R.A. van Swaaij, M. Zeman, Designing optimized nano textures for thin-film silicon solar cells, Opt. Express 21 (104) (2013) A656–A668.
[25] C. Battaglia, M. Boccard, F.-J. Haug, C. Ballif, Light trapping in solar cells: when does a Lambertian scatterer scatter Lambertianly?, J. Appl. Phys. 112 (9) (2012) 094504.
[26] S. Wiesendanger, M. Zilk, T. Pertsch, F. Lederer, C. Rockstuhl, A path to implement optimized randomly textured surfaces for solar cells, Appl. Phys. Lett. 103 (13) (2013) 131115.
[27] P. Kowalczewski, M. Liscidini, L.C. Andreani, Light trapping in thin-film solar cells with randomly rough and hybrid textures, Opt. Express 21 (105) (2013) A808–A820.
[28] Silvaco Atlas Manual, ⟨http://www.silvaco.com/products/tcad/device_simulation/atlas/atlas.html⟩, 2014.
[29] L.C. Andreani, A. Bozzola, P. Kowalczewski, M. Liscidini, Photonic light trapping and electrical transport in thin-film silicon solar cells, Sol. Energy Mater. Sol. Cells 135 (2015) 78–92.
[30] A. Richter, S.W. Glunz, F. Werner, J. Schmidt, A. Cuevas, Improved quantitative description of auger recombination in crystalline silicon, Phys. Rev. B 86 (16) (2012) 165202.
[31] A. Schenk, Finite-temperature full random-phase approximation model of band gap narrowing for silicon device simulation, J. Appl. Phys. 84 (7) (1998) 3684–3695.
[32] M. Taguchi, A. Yano, S. Tohoda, K. Matsuyama, Y. Nakamura, T. Nishiwaki, K. Fujita, E. Maruyama, 24.7% record efficiency HIT solar cell on thin silicon wafer, IEEE J. Photovoltaics 4 (2014) 96.
[33] O.D. Miller, E. Yablonovitch, S.R. Kurtz, Strong internal and external luminescence as solar cells approach the Shockley–Queisser limit, IEEE J. Photovoltaics 2 (3) (2012) 303–311.
[34] A. Ingenito, O. Isabella, M. Zeman, Nano-cones on micro-pyramids: modulated surface textures for maximal spectral response and high-efficiency solar cells, Prog. Photovoltaics: Res. Appl. (2015), http://dx.doi.org/10.1002/pip.2606.
[35] M.A. Green, K. Emery, Y. Hishikawa, W. Warta, E.D. Dunlop, Solar cell efficiency tables (version 45), Prog. Photovoltaics: Res. Appl. 23 (1) (2015) 1–9.
[36] O. Malinkiewicz, A. Yella, Y.H. Lee, G.M. Espallargas, M. Graetzel, M. K. Nazeeruddin, H.J. Bolink, Perovskite solar cells employing organic charge-transport layers, Nat. Photonics 8 (2) (2014) 128–132.
[37] T.P. White, N.N. Lal, K.R. Catchpole, Tandem solar cells based on high-efficiency c-Si bottom cells: top cell requirements for >30% efficiency, IEEE J. Photovoltaics 4 (1) (2014) 208–214.
[38] C.D. Bailie, M.G. Christoforo, J.P. Mailoa, A.R. Bowring, E.L. Unger, W.H. Nguyen, J. Burschka, N. Pellet, J.Z. Lee, M. Grätzel, et al., Semi-transparent perovskite solar cells for tandems with silicon and cigs, Energy Environ. Sci. 8 (2015) 956–963.
[39] P. Loper, B. Niesen, S. Moon, S. Martin de Nicolas, J. Holovsky, Z. Remes, M. Ledinsky, F. Haug, J. Yum, S. De Wolf, et al., Organic–inorganic halide perovskites: perspectives for silicon-based tandem solar cells, IEEE J. Photovoltaics 4 (2014) 1545.
[40] N.W. Ashcroft, N.D. Mermin, Solid State Physics, Brooks/Cole, 1976.